Emergence of Chemical Oscillations from Nanosized Target Patterns

Cédric Barroo,[1,2,5,*] Yannick De Decker,[2,3] Thierry Visart de Bocarmé,[1,2] and Norbert Kruse[1,2,4,†]
[1]Chemical Physics of Materials and Catalysis, Université libre de Bruxelles, CP243, 1050 Brussels, Belgium
[2]Interdisciplinary Center for Nonlinear Phenomena and Complex Systems (CENOLI), Université libre de Bruxelles, 1050 Brussels, Belgium
[3]Non Linear Physical Chemistry Unit, Université libre de Bruxelles, CP231, 1050 Brussels, Belgium
[4]Voiland School of Chemical Engineering and Bioengineering, Washington State University, Pullman, Washington 99164, USA
[5]Present address: School of Engineering and Applied Sciences, Harvard University, Cambridge, Massachusetts 02138, USA
(Received 21 April 2016; published 28 September 2016)

This work investigates experimentally the mechanism by which chemical oscillations emerge in a nanometric system. We monitor the spatiotemporal dynamics of an oscillating reaction on the surface of a nanosized three-dimensional Pt model catalyst. Using high-resolution field emission techniques, we are able to show that the oscillations are generated by nanoscale chemical target patterns of much shorter characteristic time than the period with which the oscillations occur. Our observations are made for a specific reaction system—NO_2 reduction with hydrogen—and represent the first experimental evidence for the presence of target patterns at the nanoscale. They can be seen as an experimental demonstration of reaction-diffusion mechanisms to hold at the nanoscale as they do at the macroscale. These results shed new light on the emergence of complexity through different time and length scales.

DOI: 10.1103/PhysRevLett.117.144501

Far from thermodynamic equilibrium, chemical reactions can exhibit time and space symmetry breaking for which dissipative phenomena such as periodic oscillations [1–4] and associated periodic chemical waves [5–7] are well-known examples. These phenomena have been observed in a variety of situations including reactions in aqueous phase [8,9], heterogeneous catalysis [10–14], or biological systems [15]. In recent years, the focus has been put on the conditions under which these behaviors can be found at very small scales. This question is central to understand the dynamics of reactive microsystems, including biological cells or dynamically responsive solid nanoparticles.

The factors controlling the importance of fluctuations in chemical oscillations have been thoroughly characterized from a theoretical point of view [16]. It was shown that the number of molecules participating in a reaction is a critical parameter leading to the conclusion that oscillations should not be expected in nanometric systems. Nevertheless, regular periodic behaviors have been imaged and characterized at such scales, for example, during the $NO_2 + H_2$ reaction on three-dimensional platinum nanocrystals [17]. These results suggest that a mechanism exists which ensures the robustness of oscillations at very small scales.

In this work, we elucidate the nature of this mechanism for the above-mentioned oscillating $NO_2 + H_2$ reaction by using high resolution field emission techniques [1]. We show that the oscillations emerge thanks to the coupling of even smaller and faster nonlinear phenomena. The ignition of the reaction occurs locally on small metal facets that produce chemical target patterns with nanometer-wide fronts propagating over short time scales ($\sim 10^{-3}$ s). These facets communicate with each other to collectively generate the previously reported oscillations, the period of which is much longer ($\sim$1 s). These results demonstrate that nonequilibrium systems can present a sort of *recursive pattern* of dissipative phenomena spanning over different spatiotemporal scales.

For the present study, platinum samples are conditioned as sharp tips that mimic the size and shape of single nanoparticles encountered in supported catalysts. The (quasi)hemispherical apex of such tips has a radius of less than 30 nm and presents different facets corresponding to different crystallographic orientations. The sample can be imaged with atomic resolution by field ion microscopy (FIM), as depicted in Fig. 1(a), with the corresponding ball model in Fig. 1(b) highlighting the morphological and surface topographical features of the sample. The sample can also be imaged with nanoscale resolution either at low temperature or under reaction conditions by field emission microscopy (FEM) [Fig. 1(c)]. A mixture of the two reacting gases is admitted to the microscope chamber, which is run as an open reactor, and the changes in the field emission patterns are monitored in real time. A description of the experimental procedure can be found in the Supplemental Material [18].

We focus on a parametric domain where regular periodic oscillations of brightness can be observed in the FEM mode [21]. The oscillations are initiated by first introducing NO_2 into the microscope chamber, which results in a decrease of the overall image brightness. The same trend has been observed in the presence of pure oxygen [22], which leads us to conclude that adsorbed oxygen species are most likely

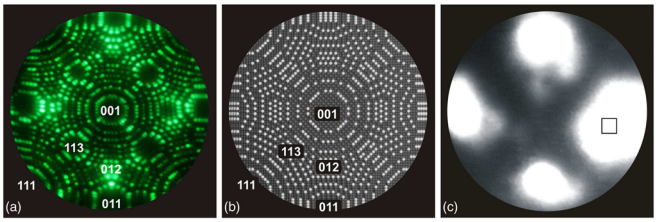

FIG. 1. Characterization of the sample: (a) Field ion micrograph of a pure (001)-oriented Pt sample with the main Miller indices (conditions: temperature $T = 60$ K, Ne pressure $P_{Ne} = 2 \times 10^{-3}$ Pa, static electric field intensity $F \sim 35\,\mathrm{V\,nm^{-1}}$). (b) Ball model of a face-centered cubic crystal lattice shaped as a quasihemisphere. The most protruding atoms, corresponding to kinks and step positions, are colored white. (c) Field emission pattern during NO_2 hydrogenation at 390 K exhibiting fast ignition of the reaction ($F \sim 4\,\mathrm{V\,nm^{-1}}$). The small square indicates the region of interest and is focused on a facet with {012} symmetry.

responsible for this brightness change. After the subsequent addition of hydrogen, the brightness starts fluctuating around the background value until a threshold H_2 pressure is reached [23]. Once this critical value has been exceeded, periodic oscillations of the brightness appear on some of the crystallographic orientations. With a 40 ms temporal resolution, all the facets involved seem to ignite simultaneously. These facets are located along the ⟨010⟩ zone lines connecting the {011} facets to the central (001) pole. As an example, Fig. 2 shows the time series of the brightness of a region of interest (ROI) centered on a {012} facet. The oscillations remain regular for hours under constant control parameters.

The robustness of the oscillations is unexpected in view of the small size of the facets where they take place; these facets contain up to ∼100 adsorbed molecules each. This suggests that a coupling mechanism exists between the different facets. Gas-phase coupling is unlikely to play a decisive role here. FEM experiments are conducted under isothermal conditions and at low pressures, so that the mean free path of molecules in the gas phase is by orders of

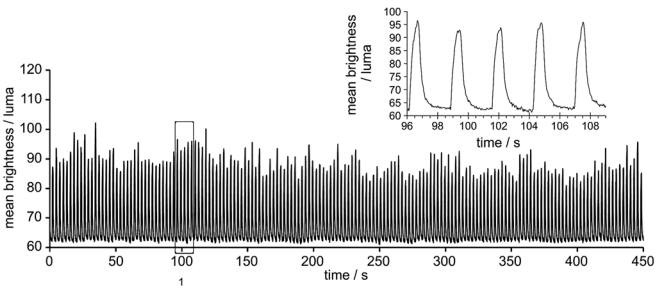

FIG. 2. Brightness signal of the self-sustained periodic oscillations probed on a region of approximately 10 nm^2 corresponding to a {012} facet. Inset: representative oscillation peaks ($T = 390$ K, $F \sim 4\,\mathrm{V\,nm^{-1}}$, partial pressures $P_{H_2} = 1.05 \times 10^{-2}$ Pa, $P_{NO_2} = 3.64 \times 10^{-4}$ Pa).

magnitude larger than the typical size of the microscope (∼20 cm diameter). The fast propagation of heat waves as phonons inside the bulk of the sample also excludes any coupling between facets via heat transfer [24]. Instead, the robustness of the oscillations is expected to be due to a spatial coupling by surface diffusion.

To characterize the coupling between facets, additional experiments are performed with a camera with very high temporal resolution; rather than monitoring dynamic processes with 50–100 fps, as previously available, 10 000 fps (and higher) are now being used and allow entering the lower microsecond time scale. A (111)-oriented Pt sample [see Fig. 3(a)] is used for these experiments. To provide a guide to the eye, the low-temperature FIM micrograph is superimposed to the FEM reaction pattern at 390 K. The active {011} facets appear bright. The different ROIs used for brightness analyses are presented in Fig. 3(b) and cover all three {011} facets and their close neighbors. Figures 3(c) and 3(d) show the sequence of ignition with a temporal resolution of 0.1 ms. The facets ignite in a sequential manner. To estimate the delay between two different facets, a threshold value of the brightness is defined as the time at which the increasing part of the brightness peak reaches a value of 10 units of brightness above the background signal. The full gray scale contains 256 steps in these experiments. This definition provides

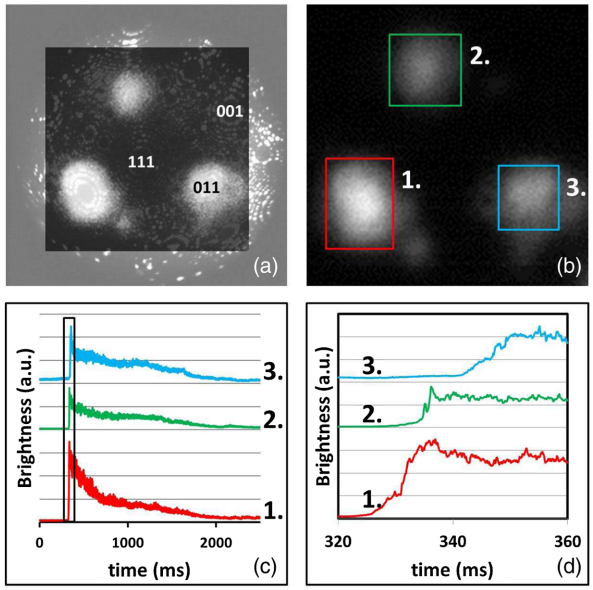

FIG. 3. Coupling via diffusion: (a) Low-T FIM pattern and high-T FEM pattern during the $NO_2 + H_2$ reaction (the field of view of the micrograph corresponds to ≈50 nm. (b) FEM pattern along with probed ROIs for brightness analysis. (c) Brightness signal of a single explosive ignition monitored in three different ROIs covering. (d) A close-up on the signals showing the delays between ignitions in the different ROIs. Conditions: frame rate=10 000 fps, $T = 390$ K, $F = 4\,\mathrm{V\,nm^{-1}}$, $P_{H_2} = 3.6 \times 10^{-3}$ Pa, $P_{NO_2} = 1.43 \times 10^{-4}$ Pa.

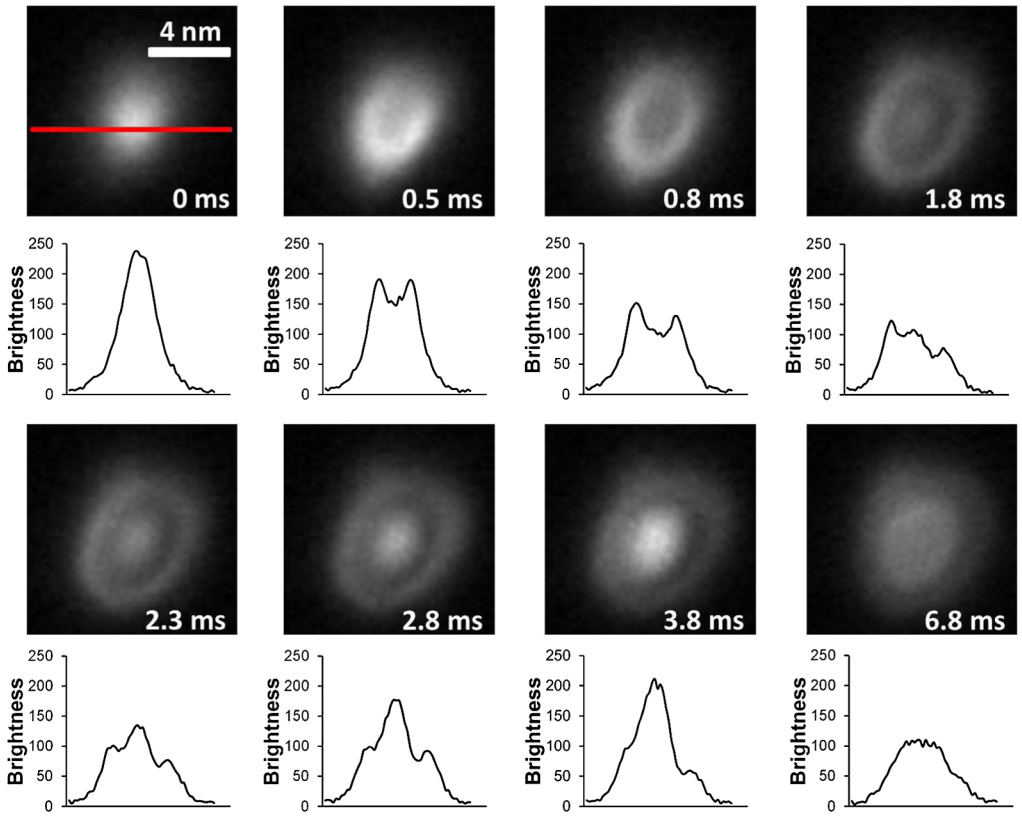

FIG. 4. Nanoscale target patterns: Sequence of FEM patterns of a {011} facet [ROI 2 in Fig. 2(b)] and corresponding line profiles of the brightness during the explosive ignition. Conditions: frame rate=10,000 fps, $T = 390$ K, $F = 4$ V nm^{-1}, $P_{H_2} = 3.6 \times 10^{-3}$ Pa, $P_{NO_2} = 1.43 \times 10^{-4}$ Pa.

delay times of (8 ± 4) ms for the ignition between ROI 1 and ROI 2 and (14 ± 4) ms between ROI 2 and ROI 3, respectively. The total time lag between ignition in ROI 1 and in ROI 3 is (22 ± 4) ms. Note that the uncertainties in delay times are related to the analysis of ignition in different experiments.

These delay times point towards a spatial coupling by *reaction diffusion*. Indeed, since the distance between the centers of two different {011} facets is ~21 nm, the coupling propagates with an effective velocity of ~2 μm s^{-1}. This value is close to the velocity of reaction-diffusion fronts observed for other similar surface reactions in similar conditions, such as the $CO + O_2$ reaction on Pt single crystals and tips (front velocity between 0.5 and 46 μm s^{-1}) [24–27]. A more detailed analysis of the very first moments of the explosive ignition inside the {011} facets confirms that nanometric chemical waves are indeed propagating on the surface. However, these fronts evolve over spatial and temporal scales that differ markedly from those of the global oscillations.

Several FEM snapshots of the upper {011} facet are presented in Fig. 4 along with the line profile of brightness probed at the center of the facet. At $t = 0$ ms, the reaction is triggered in the center of the facet and accompanied by an increase of the local brightness. The brightness signal then propagates isotropically, in the form of a ringlike feature, towards the border of the facet while the center darkens. The line profiles indicate that a peak splitting occurs after ~0.5 ms. The wave propagates towards the facet ledges where it halts for times between 1.8 and 3.8 ms. Approximately 1.8 ms after triggering the first reaction front, a second reactive burst can be seen to develop in the center of the facet. The corresponding brightness of this burst first increases and then spreads over the facet. The overall brightness signal subsequently blurs to become almost uniform (see Fig. 4 after 6.8 ms). Eventually, the overall brightness fades away over longer time scales (in the range of a few seconds). This ignition-propagation-re-ignition phenomenon is seen in more than 50% of the experiments. In some cases, similar dynamics can be observed on the three {011}. In other instances only one facet shows propagating fronts, while the other two ignite homogeneously. It has to be noted that the ignition of waves occasionally occurs at different regions which are, within the resolution of the microscope, supposed to be the border of the facet.

The succession of propagating rings is reminiscent of a macroscopic reaction-diffusion behavior known as target patterns. Target patterns are a typical feature of two-dimensional excitable systems. In such systems, local

pacemakers induce a pulse of concentration which then propagates in the form of a wave [28]. These pacemakers are usually associated with impurities or (in the case of surface reactions) with larger-size defect structures [29]. In view of the small size of the facets under investigation, it is likely that intrinsic statistical fluctuations in the density of adsorbed species are responsible for triggering the scenario [30]. Further experimental investigations are necessary to confirm that the local dynamics are indeed of the excitable type. However, we already note that coupled excitable systems can, in theory, lead to globally periodic behaviors with a quite different time scale, which is qualitatively consistent with our observation of target-pattern-induced global oscillations.

Analysis of Fig. 4 shows that the velocity of the wave front is $\sim 2\ \mu\mathrm{m\,s^{-1}}$. This value is similar to the propagation speed between different {011} facets and indeed implies that a reaction-diffusion process is at play. It also suggests that the waves observed *in* the facets are responsible for the coupling *between* facets. Our observations would thus appear to be interpreted as the nanoscale equivalent of target patterns for which the center of the nano-sized facets is the prime location for the onset of the process.

This hypothesis is supported by the fact that the characteristics of the observed nanosized waves agree qualitatively with the predictions of a simple reaction-diffusion system. We expect that the dissociative adsorption of NO_2 on the surface produces NO(ads) and O(ads), while the adsorption of H_2 leads to H(ads). NO(ads) itself can dissociate to O(ads) and N(ads). The latter has a low binding energy on Pt and therefore readily recombines to quickly desorbing N_2 species. We thus expect the kinetics to be dominated by the reaction between O(ads) and H(ads) to water. A more detailed description of mechanism can be found in the Supplemental Material [18]. This hypothesis is consistent with the sharp increase of brightness observed in the experiments: Water is indeed known to increase the image brightness in FEM on Pt [22,31]. Moreover, H_2O (ads) itself desorbs rapidly, which frees empty sites where additional gas species can adsorb. The formation of water is thus autocatalytic. The velocity of a propagating wave induced by such an autocatalytic reaction is expected to scale like

$$v \propto \sqrt{D_O k_R},$$

where D_O is the diffusion coefficient of the least mobile adsorbate [O(ads)] and k_R is the net reaction rate constant. Since $D_O \approx 10^{-13}\ \mathrm{cm^2\,s^{-1}}$ at 390 K on Pt(110) [28] and the reaction rate constant for water formation is $k_R \approx 5\times 10^5\ \mathrm{s^{-1}}$ [32], the reaction-diffusion approach predicts $v \approx 2\ \mu\mathrm{m\,s^{-1}}$, which is in very good agreement with our observations.

Similar arguments may be used to estimate the width of the corresponding reaction-diffusion pulse, for which the surface lifetime and diffusion coefficient of the main inhibitor of reaction are needed. The thermal desorption of NO(ads) is rather slow at 400 K on stepped Pt surfaces [33] and we expect this species to inhibit the reaction by blocking adsorption sites. Its lifetime is determined by the inverse of its decomposition rate constant, $k_{\mathrm{dis}} \approx 10\ \mathrm{s^{-1}}$ [34] and its diffusion coefficient has been experimentally determined to be $D_{\mathrm{NO}} = 2\times 10^{-13}\ \mathrm{cm^2/s}$ at a similar temperature on Pt(100) facets [35]. The diffusion length of the inhibitor can thus be estimated as $\sqrt{D_{\mathrm{NO}}/k_{\mathrm{dis}}} \approx 1\,\mathrm{nm}$, which is consistent with the width of the leading front of pulses observed in the experiments.

To summarize, we have investigated the reasons behind the unexpected regularity of chemical oscillations at the nanometer scale for a model surface reaction system. We used to this end an innovative approach combining the high spatial resolution of field emission techniques with the high temporal resolution of a high-speed video camera. While the highly regular periodic oscillations are rather slow (period of a few seconds) and involve the entire nanosized crystal, the system is found to produce rapidly pulsating chemical waves which propagate over nanometric distances inside small facets and create target patterns. Isotropic wave front propagation to facet ledges occurs within 2 ms. The different active facets subsequently couple via surface diffusion through fronts propagating with a similar velocity. Synchronizing the entire nanocrystal surface takes between 20 and 30 ms, which is the time needed to reach the maximum of a single peak in the global (slow) oscillations. The different facets then recover their initial state in a simultaneous fashion, which corresponds to a decrease of the global signal to its minimal value.

Our study demonstrates a coherent picture in which spatiotemporal organization occurs at all the investigated length and time scales. These results suggest that at least some of the nonlinear dynamical behaviors observed on our scale could be the result of the interplay of smaller scale dissipative phenomena, which, by interacting with each other, manage to emerge through multiple scales, from the bottom up.

C. Barroo thanks the Fonds de la Recherche Scientifique (F. R. S.-FNRS) for financial support (Ph.D. grant). The authors gratefully thank the Van-Buuren Foundation for financial support for the acquisition of equipment and the Wallonia-Brussels Federation (Action de Recherches Concertées n°AUWB 2010–2015/ULB15).

*Corresponding author.
cbarroo@ulb.ac.be
†Corresponding author.
norbert.kruse@wsu.edu

[1] C. Barroo, Y. De Decker, T. Visart de Bocarmé, and N. Kruse, J. Phys. Chem. C **118**, 6839 (2014).
[2] R. Imbihl, Surf. Sci. **603**, 1671 (2009).

[3] M. Slinko, T. Fink, T. Löher, H. H. Madden, S. J. Lombardo, R. Imbihl, and G. Ertl, Surf. Sci. **264**, 157 (1992).
[4] J.-S. McEwen, P. Gaspard, T. Visart de Bocarmé, and N. Kruse, Proc. Natl. Acad. Sci. U.S.A. **106**, 3006 (2009).
[5] N. Gottschalk, F. Mertens, M. Bär, M. Eiswirth, and R. Imbihl, Phys. Rev. Lett. **73**, 3483 (1994).
[6] S. Nettesheim, A. von Oertzen, H.-H. Rotermund, and G. Ertl, J. Chem. Phys. **98**, 9977 (1993).
[7] R. Imbihl, Non-linear dynamics in catalytic reactions, in *Handbook of Surface Science*, edited by E. Hasselbrink and B. I. Lundqvist (Elsevier B.V., Amsterdam, 2008), p. 342.
[8] B. P. Belousov, A periodic reaction and its mechanism., in *Autowave Processes in Diffusion–Reaction Systems* (Gorky State University, Gorky, 1951), p. 76.
[9] A. M. Zhabotinskii, Biophysics **9**, 329 (1964) [Biofizika **9**, 306 (1964)].
[10] Th. Schmidt, A. Schaak, S. Günther, B. Ressel, E. Bauer, and R. Imbihl, Chem. Phys. Lett. **318**, 549 (2000).
[11] F. Esch, S. Günther, E. Schütz, A. Schaak, I. G. Kevrekidis, M. Marsi, M. Kiskinova, and R. Imbihl, Catal. Lett. **52**, 85 (1998).
[12] M. F. H. van Tol, A. Gielbert, and B. E. Nieuwenhuys, Catal. Lett. **16**, 297 (1992).
[13] V. V. Gorodetskii, J. Lauterbach, H.-H. Rotermund, J. H. Block, and G. Ertl, Nature (London) **370**, 276 (1994).
[14] H.-H. Rotermund, Surf. Sci. **386**, 10 (1997).
[15] A. Goldbeter, Curr. Biol. **18**, R751 (2008).
[16] P. Gaspard, J. Chem. Phys. **117**, 8905 (2002).
[17] C. Barroo, Y. De Decker, T. Visart de Bocarmé, and P. Gaspard, J. Phys. Chem. Lett. **6**, 2189 (2015).
[18] See Supplemental Material at http://link.aps.org/supplemental/10.1103/PhysRevLett.117.144501 for a description of the experimental procedure, and a more detailed description of the mechanism, which includes Refs. [19,20].
[19] D. Brown, Tracker Video Analysis and Modeling Tool, Version 4.80 (2009), http://physlets.org/tracker/.
[20] J.-S. McEwen, P. Gaspard, Y. De Decker, C. Barroo, T. Visart de Bocarmé, and N. Kruse, Langmuir **26**, 16381 (2010).
[21] Y. S. Lim, M. Berdau, M. Naschitzki, M. Ehsasi, and J. H. Block, J. Catal. **149**, 292 (1994).
[22] P. T. Dawson and Y. K. Peng, Surf. Sci. **92**, 1 (1980).
[23] C. Barroo, S. V. Lambeets, F. Devred, T. D. Chau, N. Kruse, Y. De Decker, and T. Visart de Bocarmé, New J. Chem. **38**, 2090 (2014).
[24] V. V. Gorodetskii, J. H. Block, W. Drachsel, and M. Ehsasi, Appl. Surf. Sci. **67**, 198 (1993).
[25] M. P. Cox, G. Ertl, and R. Imbihl, Phys. Rev. Lett. **54**, 1725 (1985).
[26] S. Jakubith, H.-H. Rotermund, W. Engel, A. von Oertzen, and G. Ertl, Phys. Rev. Lett. **65**, 3013 (1990).
[27] M. Ehsasi, A. Karpowicz, M. Berdau, W. Engel, K. Christmann, and J. H. Block, Ultramicroscopy **49**, 318 (1993).
[28] J. V. Barth, Surf. Sci. Rep. **40**, 75 (2000).
[29] M. Bär, Ch. Zülicke, M. Eiswirth, and G. Ertl, J. Chem. Phys. **96**, 8595 (1992).
[30] C. Reichert, J. Starke, and M. Eiswirth, J. Chem. Phys. **115**, 4829 (2001).
[31] V. V. Gorodetskii, J. H. Block, and W. Drachsel, Appl. Surf. Sci. **76–77**, 129 (1994).
[32] A. G. Makeev and B. E. Nieuwenhuys, J. Chem. Phys. **108**, 3740 (1998).
[33] N. Kruse, G. Abend, and J. H. Block, J. Chem. Phys. **88**, 1307 (1988).
[34] N. Kruse and J. H. Block, Stud. Surf. Sci. Catal. **30**, 173 (1987).
[35] E. S. Kurkina, A. V. Malykh, and A. G. Makeev, Computational Mathematics and Modeling **10**, 363 (1999).